Frequency Stability and Noise Characteristics of Ultra-High Frequency (UHF) Nanoelectromechanical Resonators

X.L. Feng* and M.L. Roukes**

*Electrical Engineering, **Applied Physics, Physics & Bioengineering
California Institute of Technology, MC 114-36
Pasadena, CA 91125, USA, *Email: xfeng@caltech.edu

ABSTRACT

Nanoelectromechanical silicon carbide doubly-clamped beam vibrating resonators operating in the ultra-high frequency (UHF) band, with resonance frequencies of 395MHz, 411MHz, 428MHz, and 482MH, and quality factors (Q's) of 2000~3000, have been demonstrated. The readout of electromechanical resonances from the nanodevices is integrated with a low-noise phase-locked loop to implement *real-time* resonance frequency locking and tracking, with which the frequency stability and phase noise of the resonators are measured. The measured frequency stability shows typical crystal resonator behavior, and represents *unprecedented* mass sensitivity (in 10^{-20}g ~ 10^{-21}g scale) achieved by nanoelectromechanical resonant mass sensors. The achievable lowest phase noise of the system is ultimately determined by the thermomechanical noise of the resonator device, but presently limited by the thermal noise and other noise processes of the measurement electronic system.

Keywords: nanoelectromechanical systems, resonator, mass sensor, frequency stability, phase noise

1 INTRODUCTION

Nanoelectromechanical systems (NEMS) are emerging as great candidates for a variety of technological applications ranging from sensors and actuators to signal processing and communications [1]. Within the past decade, it has already been firmly established that advances in the mainstream microelectromechanical systems (MEMS), as enabling technologies, are demonstrating immense potentials for signal processing and communications based on micromachined devices and systems [2]. Facilitated by the advanced nanofabrication technologies, as the MEMS devices are scaled down into their NEMS counterparts, smaller device size and mass, lower power consumption, higher operating frequencies, higher responsivity and sensitivity, and other superb properties are attained [1]. In particular, nanofabricated electromechanical resonators (i.e., NEMS resonators) routinely operate at higher frequencies (often in the VHF and UHF bands) than their MEMS counterparts do. Therefore, radio-frequency (RF) NEMS resonators are promising to be the future on-chip high-Q resonators for frequency generation and conversion in RF electronics and wireless communication systems. Moreover, NEMS resonators' high operating frequencies, small mass, and high-Q's, also make them natural choices for resonant mass and force sensors with ultrahigh sensitivities [3,4], and for approaching quantum limits in fundamental physics measurements [5,6]. In almost all these cases, high-frequency, high-Q and low-noise operation are desirable, while on the other hand the implementations with nanoscale devices impose tremendous challenges. Thus, new and elaborate engineering is *crucial* to realize the above projected applications with NEMS resonators. Particularly, as the ultimate performance of NEMS is limited by various fundamental noise processes [7], it is of significance to get a comprehensive understanding of the frequency stability and noise processes of NEMS resonators. In this work, we present the initial experimental study of frequency stability and phase noise of UHF NEMS resonators.

2 UHF NEMS RESONATOR DEVICES

In order to make high-frequency mechanical resonators, it is favorable to choose materials with high modulus-to-density ratios, as resonance frequencies of most flexural modes follow $f \propto \sqrt{E/\rho}$, with E the elastic modulus and ρ the density. Hence, new promising materials such as SiC, diamond, and carbon nanotubes are better choices than conventional Si and GaAs in achieving higher-operating frequencies. In the present study, monocrystalline 3C silicon carbide (3C-SiC) thin layer epitaxially grown on silicon is used as the structural material of the vibrating UHF NEMS resonator devices, as it has been proven to be remarkably suitable for making UHF NEMS resonators [8]. The device nanofabrication process, as described in detail in [9], consists of definition of micron-scale by photolithography, the pattern transfer of the nanoscale device via electron-beam lithography and metallization, and finally a two-step electron-cyclotron resonance (ECR) plasma etching to suspend the NEMS device. To minimize the mass loading effect upon the SiC structural layer and to facilitate UHF operation, 10nm Ti atop of 30nm Al is used as metallization layer, instead of the widely used but much heavier Au. Ti layer is used as a passivation to prevent the oxidation of Al.

The NEMS resonator devices are designed to be doubly-clamped beams as this simple design allows for better geometry and dimension control, and thus relatively

accurate resonance frequency control in fabricating a family of UHF devices for a collective and comparative study. The specs of these devices are summarized in Table 1 (a VHF device, at 295MHz, is also included).

Table 1: UHF NEMS Resonator Devices Specs.

Resonance Frequency (MHz)	Length (μm)	Width (nm)	Thickness (nm)	Device Mass (fg, 10^{-15}g)
295	2.65	180	80	158.3
395	1.75	120	80	74.4
411	1.7	120	80	72.3
420	1.8	150	100	103.6
428	1.65	120	80	75.5
482	1.55	120	80	70.9

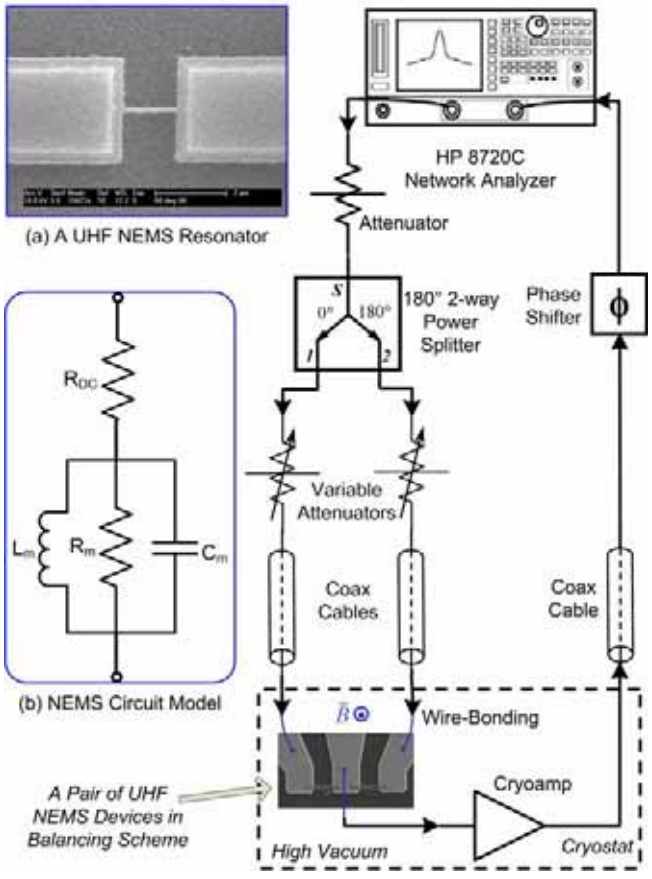

Figure 1: Schematic of the electromechanical resonances readout scheme, with a balanced electronic detection circuit specifically modified and optimized for UHF NEMS. *Inset (a)*: SEM image of a typical UHF SiC NEMS (top view, the etched undercut indicating that device is freely suspended). *Inset (b)*: the parallel LRC tank circuit model for a magnetomotively-transduced NEMS. The total impedance of the device includes the DC impedance R_{DC} and the electromechanical impedance $Z_m(=R_m//(1/j\omega C_m)//j\omega L_m)$.

The NEMS resonators are actuated and the resonance signals are detected with the magnetomotive transduction scheme [10], in which the NEMS devices are preserved in high vacuum (<10^{-7} Torr) and cryogenically cooled down in liquid helium where a superconducting magnet provides the strong magnetic field for the magnetomotive transduction. In this work, all samples are positioned so that the magnetic field is perpendicular to the sample plane, and in-plane fundamental flexural mode is excited and picked up for all NEMS devices. To date, it is still only magnetomotive transduction that has successfully allowed nanomechanical resonators to operate in the UHF band.

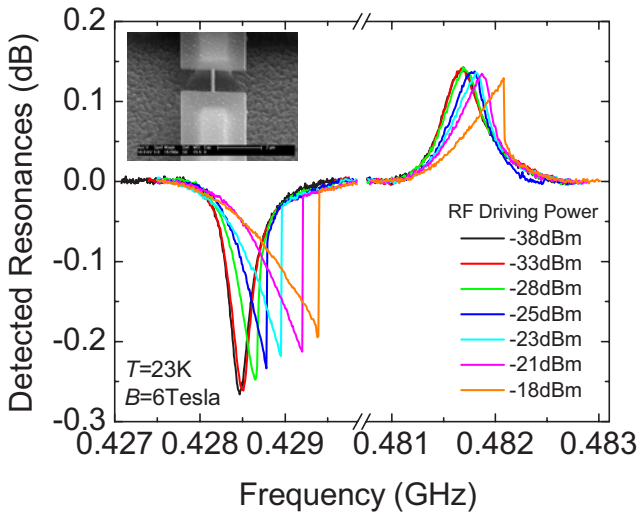

Figure 2: Detected electromechanical resonances of a pair of NEMS resonators, at 428MHz (Q~2500) and 482MHz (Q~2000) respectively. Shown are the resonance curves as the driving RF power is increased. *Inset*: SEM image (tilted view) showing the suspension of a typical UHF NEMS.

To read out the vanishingly-small resonances signals from these tiny UHF NEMS devices (the signal amplitude decreases as the device size decreases), the basic idea of a prototype balanced-bridge detection circuit [11] (initially demonstrated for HF and VHF NEMS) is implemented, modified and engineered specifically for the readout of UHF electromechanical resonances. As shown in Figure 1, the source RF power from the network analyzer (HP 8720C) is split into out-of-phase two branches to drive the two devices which have been deliberately designed to have different but close dimensions to attain different resonance frequencies as well as close DC impedance, for better impedance balancing between the two branches off the resonances. Variable attenuators are applied in each branch to attain better balancing, as the differences in the coax cable and other components between both branches always induce amplitude and phase change. With the background signal (off resonances signal, arising from the embedding impedances of the measurement system) minimized by this balancing scheme (ideally, off resonances background should be at *virtual ground*, i.e., -∞ dB in transmission S_{21}),

the vanishingly-small resonances signals become visible (better than those from the direct measurements of reflection or transmission with only one single device) and it is possible to extract the resonances and process them to realize more advanced functions.

Figure 2 shows the detected resonances signals from the pair of 428MHz and 482MHz devices. The off-resonances background signal has been subtracted and the plotted resonances curves reflect the fact that the devices are driven out-of-phase. It is also shown that as the RF power sent to the device is increased, the device is driven into nonlinear regime. From the experimental data, the onset of nonlinearity for the 428MHz device is about -28dBm, while that for the 482MHz device is about -18dBm. This is because the shorter the beam, the stiffer it is and the higher power it can handle. Moreover, the smaller resonance peak of the 482MHz is also because the device is shorter and stiffer as compared with the 428MHz device.

3 FREQUENCY STABILITY

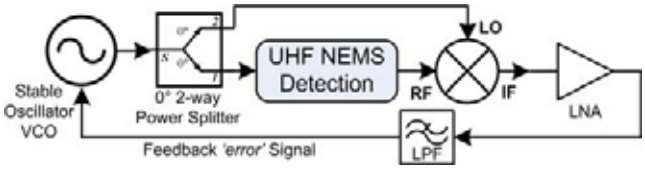

Figure 3: UHF NEMS detection integrated with low-noise phase-locked loop for precise NEMS resonance frequency locking and tracking in *real-time*.

Among many engineering challenges to boost NEMS for more practical applications, it is of great importance to develop the generic protocol of integrating NEMS resonators with feedback and control systems. Low-noise, precise and reliable frequency locking and tracking are the keys for *real-time resonant sensing* applications. With the extraction of UHF resonances signals addressed above, it becomes possible to apply feedback and control upon the NEMS resonances signals. As shown in Figure 3, we have successfully demonstrated a low-noise phase-locked loop (PLL) integrated with UHF NEMS, which is an upgraded version of the VHF NEMS-PLL system [12].

Frequency stability of the NEMS resonators is measured with the NEMS-PLL system at stabilized temperatures. A universal counter (Agilent 53132A) is used to carry out this time-domain measurement, and the frequency stability is evaluated by the statistics of the measurement ensemble. A widely-used criterion for frequency stability (or, instability) is the Allan deviation [7,13]. For a finite measurement ensemble with N samples, the Allan deviation is ($1/\sqrt{2}$ times the standard deviation of the fractional frequency variation)

$$\sigma(\tau) \cong \frac{1}{\sqrt{2}} \left[\frac{1}{N} \sum_{i=1}^{N} \left(\frac{\bar{f}_{i+1} - \bar{f}_i}{f_0} \right)^2 \right]^{\frac{1}{2}}, \qquad (1)$$

where f_0 is the resonance frequency, and $\bar{f}_i$ is the measured (averaged) frequency in the ith time interval.

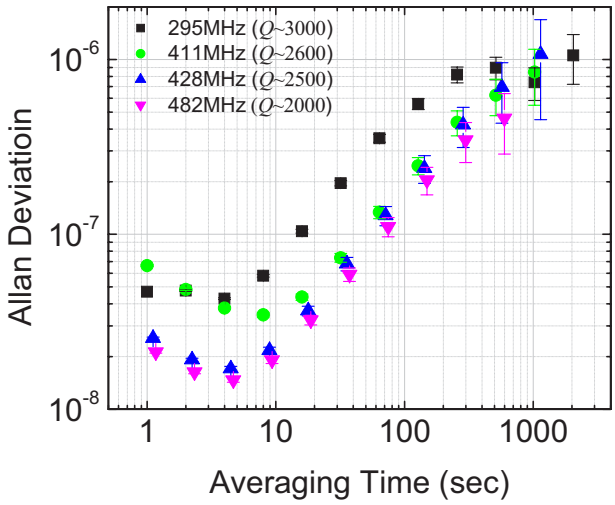

Figure 4: Measured Allan deviation data, showing the frequency stability (instability) of a family of UHF NEMS.

Table 2: Performance of UHF NEMS Resonators & PLL.

f_0 (MHz)	Q	σ (τ=1sec)	DR (dB)	Mass Sensitivity (1zg=10^{-21}g)
295	~3000	4.7×10^{-8}	80	~15 zg
420	~1200	3.1×10^{-7}	90	~67 zg
411	~2600	6.6×10^{-8}	85	~10 zg
428	~2500	2.5×10^{-8}	90	~4 zg
482	~2000	2.1×10^{-8}	98	~3 zg

As plotted in Figure 4, the measured Allan deviation as a function of averaging time, for several UHF NEMS resonators, shows the characteristics of a typical crystal resonator, with similar tendency as that of quartz crystal resonator. The data show that the short term frequency stability of the NEMS resonators is optimized to be in the 10^{-8} to 10^{-7} range, with minimum Allan deviation values at about τ=5sec averaging time for all these resonators. It is probably the most intriguing promise of these UHF NEMS-PLL systems, that the measured frequency stability is translated into *unprecedented* mass sensitivity if the devices are used as inertial mass sensors, based on the analyses in [3]. The measured Q's, Allan deviation at 1sec averaging time, achieved dynamic range for the UHF NEMS-PLL systems, and the corresponding mass sensitivity values calculated from these measured quantities, are collected in Table 2. These mass sensitivity values go deep into the *zepto-gram* (10^{-21}g) scale and again manifest that single-molecule/atom mass diction with UHF NEMS are possible and applicable. Also it is clearly verified that frequency stability and thus the overall mass sensing performance rely on a combination of high-frequency and high-Q. Therefore,

scaling up operating frequency and simultaneously retaining high-Q remains a great challenge for NEMS mass sensor engineering. Besides, to fully understand the origin and mechanism of the deteriorating long-term stability shown in Figure 4, and to develop protocols for optimizing both short-term and long-term stability, study upon various possible drifting and aging effects in the system is needed.

4 PHASE NOISE OF UHF NEMS

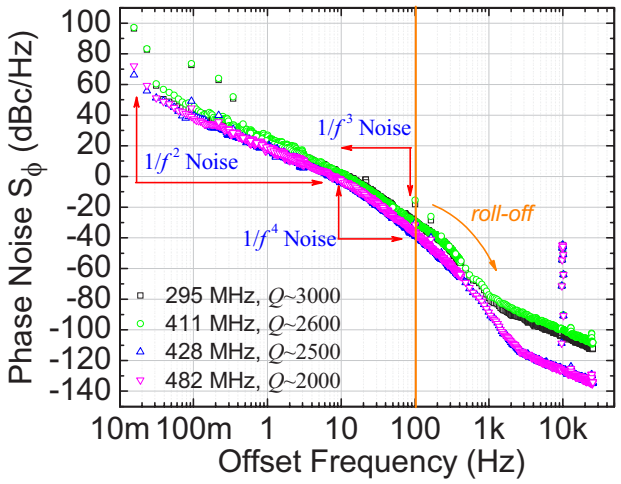

Figure 5: Phase noise performance of generations of UHF NEMS resonators. Shown are the measured phase noise spectrum curves versus offset frequency from the carrier.

The phase noise spectrum is also measured using the NEMS-PLL scheme in Figure 3. The noise spectrum of the control voltage of the VCO, $S_V(\omega)$ is directly measured by a dynamic signal analyzer (HP 35665A), at the port where the error signal is fed back to the VCO as control voltage. Hence the frequency noise spectrum of the VCO output induced by the VCO input control voltage noise is

$$S_f(\omega) = K_V{}^2 S_V(\omega), \tag{2}$$

where K_V [Hz/volt] is the gain of the VCO in the frequency modulation mode. Thus the equivalent phase noise spectrum is [13]

$$S_\phi(\omega) = \frac{1}{\omega^2} S_f(\omega), \tag{3}$$

where $\omega=2\pi f$ is the offset frequency in radius (with f in Hz). The measured phase noise as a function of offset frequency from carrier is collected in Figure 5 for several NEMS resonators. It is observed that in the range of 0.1Hz to 10Hz, the phase noise has $1/f^2$ behavior; while in the range of 10Hz to 100Hz, it approximately follows $1/f^3$ (for the 295MHz and 411MHz NEMS with PLL) or $1/f^4$ (for the 428MHz and 482MHz NEMS with PLL). The far-from-carrier roll-off is attributed to the measurement system time constant. Analyses show that the ultimate phase noise performance is limited by thermomechanical noise of the device itself; while here in the practical system, as there is a mismatch between the noise floor of the preamplifier and that of the NEMS device, the real phase noise is currently limited by the thermal noise of the preamp plus other noise processes in the measurement electronic system.

5 CONCLUSIONS

We have demonstrated generations of UHF silicon carbide NEMS resonators. The successful integration of a low-noise phase-locked loop with these resonators has been employed to directly characterize the frequency stability and phase noise performance of the NEMS. Roadmaps of Allan deviation and phase noise for 300~500MHz UHF NEMS are built. The measured frequency stability is translated into unprecedented mass sensitivity and the data show that ultrasensitive mass detection based on UHF NEMS resonators is very intriguing and is promising for approaching single-molecule/atom sensitivity. The unique NEMS-PLL integration allows for real-time, low noise detection of miniscule mass loading and fluctuation upon NEMS devices. The study shows that high-frequency and high-Q engineering is crucial for both sensitive detection and low phase noise, stable oscillator applications.

Acknowledgement: This work has been generously supported by DARPA/MTO. We thank S. Stryker for his help with the experimental apparatus.

REFERENCES

[1] M.L. Roukes, "Nanoelectromechanical Systems", *Tech. Digest of the 2000 Solid-State Sensor and Actuator Workshop* (*Hilton Head'00*) 1, 2000.
[2] C. T.-C. Nguyen, *Tech. Proceedings of the 2003 Nanotechnology Conference and Trade Show* (*Nanotech2003*) 452, 2003.
[3] K.L. Ekinci, Y.T. Yang, M.L. Roukes, *J. Appl. Phys.* **95**, 2682, 2004.
[4] K.L. Ekinci, X.M.H. Huang, M.L. Roukes, *Appl. Phys. Lett.* **84**, 4469, 2004.
[5] M.D. LaHaye, O. Buu, B. Camarota, K.C. Schwab, *Science* **304**, 74, 2004.
[6] K. Schwab, E.A. Henriksen, J.M. Worlock, M.L. Roukes, *Nature* **404**, 974, 2000.
[7] A.N. Cleland, M.L. Roukes, *J. Appl. Phys.* **92**, 2758, 2002.
[8] X.M.H. Huang, C.A. Zorman, M. Mehregany, M.L. Roukes, *Nature* **421**, 496, 2003.
[9] X.M.H. Huang, C.A. Zorman, M. Mehregany, M.L. Roukes, *Transducers'03* **1**, 722, 2003.
[10] A.N. Cleland, M.L. Roukes, *Sensors & Actuators A* **72,** 256, 1999.
[11] K.L. Ekinci, Y.T. Yang, X.M.H. Huang, M.L. Roukes, *Appl. Phys. Lett.* **81**, 2253, 2002.
[12] C. Callegari, Y.T. Yang, X.L. Feng, M.L. Roukes, *to be published*, 2005.
[13] J.A. Barnes, A.R. Chi, L.S. Cutler, *et al.*, *IEEE Trans. Instr. & Meas.* **IM-20,** 105, 1971.